

Rare and Semi-rare Decays of Beauty Mesons in ATLAS

Wolfgang Walkowiak*, on behalf of the ATLAS Collaboration

University of Siegen, 57068 Siegen, Germany

E-mail: walkowiak@hep.physik.uni-siegen.de

The ATLAS experiment at the Large Hadron Collider has performed measurements of the rare flavor-changing neutral-current processes $b \rightarrow s \mu^+ \mu^-$ and $B_{(s)}^0 \rightarrow \mu^+ \mu^-$ which are sensitive to New Physics effects. This contribution presents recent ATLAS results from the angular analysis of the $B_d^0 \rightarrow K^{*0} \mu^+ \mu^-$ decay with LHC Run 1 data, the $\mathcal{B}(B_{(s)}^0 \rightarrow \mu^+ \mu^-)$ measurement with 2015 and 2016 data as well as projections for the $B_d^0 \rightarrow K^{*0} \mu^+ \mu^-$ and $\mathcal{B}(B_{(s)}^0 \rightarrow \mu^+ \mu^-)$ measurements for the High-Luminosity LHC phase.

*18th International Conference on B-Physics at Frontier Machines - Beauty2019 -
29 September / 4 October, 2019
Ljubljana, Slovenia*

*Speaker.

1. Introduction

New physics beyond the Standard Model (SM) may manifest itself in angular distributions of $b \rightarrow s \mu^+ \mu^-$ processes or the branching fractions of very rare B meson decays. The ATLAS experiment [1] at the Large Hadron Collider (LHC) [2] at CERN performs indirect searches for New Physics by an angular analysis of the $B_d^0 \rightarrow K^{*0} \mu^+ \mu^-$ decay and measuring the branching fractions of the rare decays $B_s^0 \rightarrow \mu^+ \mu^-$ and $B^0 \rightarrow \mu^+ \mu^-$. In addition, expected sensitivities for the angular analysis in the decay channel $B_d^0 \rightarrow K^{*0} \mu^+ \mu^-$ and for the branching fractions of the rare decays $B_{(s)}^0 \rightarrow \mu^+ \mu^-$ at the High-Luminosity LHC (HL-LHC) [3] are presented.

2. Angular Analysis of $B_d^0 \rightarrow K^{*0} \mu^+ \mu^-$

Mediated by flavour-changing neutral currents (FCNC), in the Standard Model (SM) the decay $B_d^0 \rightarrow K^{*0} \mu^+ \mu^-$ with $K^{*0} \rightarrow K^+ \pi^-$ proceeds via loop diagrams. The complex angular structure of this decay is fully described by three angles and the dimuon invariant mass squared q^2 . Multiple angular observables provided by this decay are sensitive to different types of New Physics (NP). A 3.4σ deviation from SM calculations is reported by the LHCb collaboration [4]. The measurement [5] with the ATLAS detector [1], using 20.3 fb^{-1} of pp collision data at a centre-of-mass energy of $\sqrt{s} = 8 \text{ TeV}$ collected in 2012, adopts the LHCb analysis method including the definitions of angular observables and of optimised parameters $P_i^{(\prime)}$ [6]. The latter are designed to minimise uncertainties from hadronic form factors and therefore increase the sensitivity to NP. Due to the limited statistics a set of trigonometric transformations of the angular variables [6] is employed in the analysis presented.

In order to maximise the signal yield, data are combined from trigger chains with one, two or at least three identified muons. Furthermore this ensures a sensitivity of the analysis down to the kinematic threshold of $q^2 = 0.04 \text{ GeV}^2$. Signal candidates are reconstructed from two charged tracks satisfying $m_{K\pi} \in [846, 946] \text{ MeV}$ and two muons, requiring $m_{K\pi\mu\mu} \in [5110, 5700] \text{ MeV}$. Cut-based selections on the vertex fit quality $\chi^2/\text{n.d.f.} < 2$, the B^0 lifetime significance $t/\sigma_t > 12.75$, the pointing angle $\cos\theta > 0.999$ and the K^{*0} momentum $p_T(K^{*0}) > 3 \text{ GeV}$ are used to suppress the combinatorial background. This selection results in a data sample of 787 events in the signal range of $q^2 \in [0.04, 6.0] \text{ GeV}^2$. Data with a q^2 above 6 GeV^2 are excluded in order to suppress a radiative tail from $B^0 \rightarrow K^{*0} J/\psi$ events.

To extract the angular parameters an extended unbinned maximum-likelihood fit to the invariant mass $m_{K\pi\mu\mu}$ and the angular distributions $\cos\theta_K$, $\cos\theta_L$ and ϕ is performed in six bins of q^2 , with three of the bins overlapping. The fit yields a total of 342 ± 39 signal events. A distinct background contribution from $B^0 \rightarrow D^0/D_{(s)}^+ X$ decays at $\cos\theta_L \sim 0.7$ is excluded by vetoing the $D^0/D_{(s)}^+$ mass ranges. The background from fake K^{*0} candidates and $B^+ \rightarrow K^+/\pi^+ \mu^+ \mu^-$ decays, observed at $\cos\theta_K \sim 1$, is treated as a systematic uncertainty with the fake K^{*0} candidates providing the largest contribution. Overall, the measurement is largely dominated by statistical uncertainty.

Figure 1 compares the results for the P_4' and P_5' parameters to the theoretical computations of Jäger and Camalich (JC) [9, 10], Descotes-Genon et al. (DHMV) [8] and Ciuchini et al. (CFFMPSV) [7]. Experimental results from LHCb [4], CMS [11] and Belle [12] are overlaid as well. The P_4' and P_5' measurements in the $q^2 \in [4.0, 6.0] \text{ GeV}^2$ bin differ by $\sim 2.7\sigma$ from the

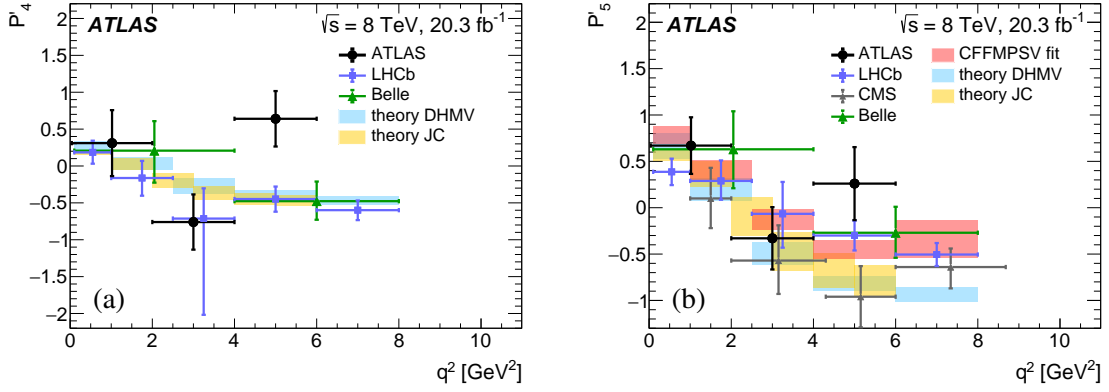


Figure 1: The measured values of P'_4 (a) and P'_5 (b) compared with predictions from the theoretical groups CFFMPSV [7] (only for P'_5), DHMV [8] and JC [9, 10]. Experimental results from LHCb [4], CMS [11] (only for P'_5) and Belle [12] are shown as well. Figures taken from [5].

DHMV model, a deviation observed similarly by the LHCb collaboration [4]. Overall, all ATLAS measurements are compatible with the different predictions at the three-standard-deviation level as well as with the results provided by the other experiments.

3. Branching fractions of $B_s^0 \rightarrow \mu^+ \mu^-$ and $B^0 \rightarrow \mu^+ \mu^-$

The rare decays $B_s^0 \rightarrow \mu^+ \mu^-$ and $B^0 \rightarrow \mu^+ \mu^-$, which are sensitive to New Physics in the decays via loop diagrams, are highly suppressed in the Standard Model (SM) with predicted branching fractions [13, 14] of $(3.65 \pm 0.23) \times 10^{-9}$ and $(1.06 \pm 0.09) \times 10^{-10}$, respectively. The ATLAS Run 1 result [15] is compatible with the SM at the 2σ level, and the $\mathcal{B}(B_{(s)}^0 \rightarrow \mu^+ \mu^-)$ values are lower than the CMS-LHCb combined result [16]. Recent measurements by the LHCb [17] and CMS [18] collaborations, including part of the Run 2 data, set upper limits of $\mathcal{B}(B^0 \rightarrow \mu^+ \mu^-) < 3.4 \times 10^{-10}$ and $\mathcal{B}(B^0 \rightarrow \mu^+ \mu^-) < 3.6 \times 10^{-10}$ at 95% confidence level (CL), respectively, which reduces the tension in this parameter.

The updated ATLAS measurement [19] of the $B_{(s)}^0 \rightarrow \mu^+ \mu^-$ branching fractions includes 36.2 fb^{-1} of data taken at a centre-of-mass energy of 13 TeV during 2015 and 2016 (LHC Run 2) and a combination with the result based on 25 fb^{-1} data taken at 7 and 8 TeV during LHC Run 1. For Run 2, events triggered by two muons ($p_T(\mu_1) > 6 \text{ GeV}$, $p_T(\mu_2) > 4 \text{ GeV}$, $|\eta| < 2.5$) with the invariant di-muon mass $m_{\mu^+ \mu^-}$ in the range of 4 to 8.5 GeV are selected. The dominant combinatorial background ($b \rightarrow \mu X \times \bar{b} \rightarrow \mu X$ pairs) is rejected by a 15-variable Boosted Decision Tree (BDT) which is trained and tested on data sidebands and simulated signal events. Tails from partially reconstructed $b \rightarrow \mu^+ \mu^- X$ decays like $B \rightarrow \mu^+ \mu^- X$, $B \rightarrow c \mu X \rightarrow s(d) \mu^+ \mu^- X$ or $B_c \rightarrow J/\psi \mu \nu$, which involve real di-muons at low $m_{\mu^+ \mu^-}$, and semi-leptonic decays ($B_{(s)}/\Lambda_b^0 \rightarrow h \mu \nu$ with $h = \pi, K, p$) contribute to the signal region and are taken into account in the signal fit. A small contribution of $B \rightarrow hh'$ ($h^{(\prime)} = \pi^\pm, K^\pm$) decays, with hadrons misidentified as muons, peaks in the $B_{(s)}^0 \rightarrow \mu^+ \mu^-$ signal region contributing 2.9 ± 2.0 events after a ‘‘tight’’ muon selection is applied. The yield in the normalisation channel $B^\pm \rightarrow J/\psi K^\pm$ with $J/\psi \rightarrow \mu^+ \mu^-$ is determined by an unbinned maximum likelihood fit to $m_{J/\psi K^\pm}$ while the efficiency relative to $B_{(s)}^0 \rightarrow \mu^+ \mu^-$ is extracted

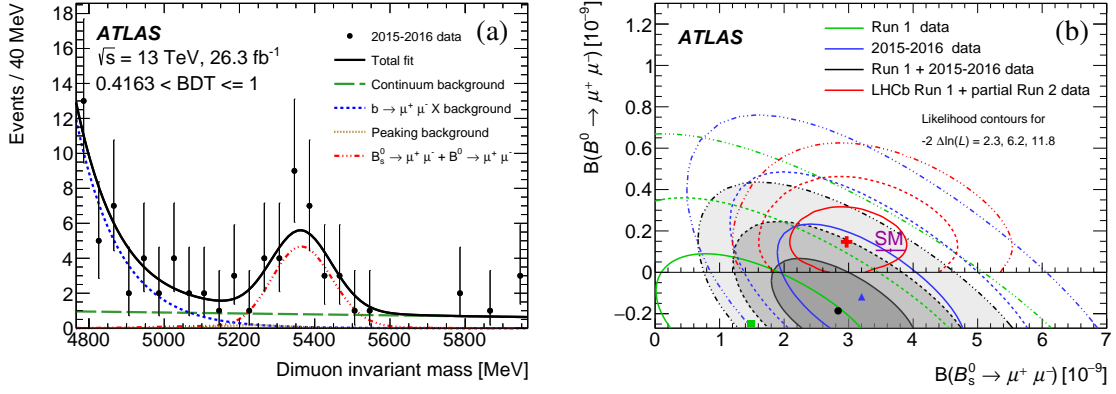


Figure 2: (a): Dimuon invariant mass distribution in the unblinded data, for the highest interval of BDT output. The result of the maximum-likelihood fit is superimposed. The total fit is shown as a continuous line, with the dashed lines corresponding to the observed signal component, the $b \rightarrow \mu^+ \mu^- X$ background, and the continuum background. The signal components are grouped in one single curve, including both the $B_s^0 \rightarrow \mu^+ \mu^-$ and the (negative) $B^0 \rightarrow \mu^+ \mu^-$ component. The curve representing the peaking $B_s^0 \rightarrow hh'$ background lies very close to the horizontal axis [19].

(b): Likelihood contours for the combination of the Run 1 and 2015–2016 Run 2 results (shaded areas). The contours are obtained with the combination of the likelihood for the two analyses, for values of $-2 \Delta \ln \mathcal{L}$ equal to 2.3, 6.2 and 11.8. The contours for the individual 2015–2016 Run 2 and Run 1 results as well as the ones from the latest LHCb result [17] are overlaid. The SM predictions and their uncertainties [13] are included. Figures taken from [19].

from Monte Carlo (MC) within a fiducial volume defined by $p_T(B) > 8 \text{ GeV}$ and $|\eta_B| < 2.5$. The overall efficiency ratio $R_\epsilon = \epsilon_{J/\psi K^\pm} / \epsilon_{\mu^+ \mu^-}$ is $0.1176 \pm 0.0009 \text{ (stat.)} \pm 0.0047 \text{ (syst.)}$ with the largest contribution to the systematic uncertainties originating from data-MC discrepancies in the BDT input quantities. A correction of 2.7% has been applied to R_ϵ to account for the effective B_s^0 lifetime.

Due to the limited mass resolution the overlapping B_s^0 and B_d^0 peaks are statistically separated by an unbinned maximum likelihood fit to the $m_{\mu^+ \mu^-}$ distributions in four BDT bins. The signal and $B \rightarrow hh'$ distributions are modelled by three double-Gaussian PDFs, each with a common mean, while the background is described by a first-order polynomial (combinatorial background) in combination with an exponential distribution ($b \rightarrow \mu^+ \mu^- X$ and semi-leptonic background) whose shape parameters and normalisations are obtained from data (Figure 2 (a)).

For the Run 2 data, yields of $N_s = 80 \pm 22 B_s^0 \rightarrow \mu^+ \mu^-$ and $N_d = -12 \pm 20 B^0 \rightarrow \mu^+ \mu^-$ events are extracted, consistent with SM expectations of $N_s^{\text{SM}} = 91$ and $N_d^{\text{SM}} = 10$, respectively. Employing a Neyman construction a branching fraction of $\mathcal{B}(B_s^0 \rightarrow \mu^+ \mu^-) = \left(3.21_{-0.91}^{+0.96} \text{ (stat.)}_{-0.30}^{+0.49} \text{ (syst.)}\right) \times 10^{-9}$ and an upper limit of $\mathcal{B}(B^0 \rightarrow \mu^+ \mu^-) < 4.3 \times 10^{-10}$ at 95% CL are obtained. A combination of the likelihood contours of the Run 2 (2015 and 2016) and Run 1 results (Figure 2 (b)) is compatible with the SM at the 2.4σ level and results in $\mathcal{B}(B_s^0 \rightarrow \mu^+ \mu^-) = \left(2.8_{-0.7}^{+0.8}\right) \times 10^{-9}$ and $\mathcal{B}(B^0 \rightarrow \mu^+ \mu^-) < 2.1 \times 10^{-10}$ at 95% CL.

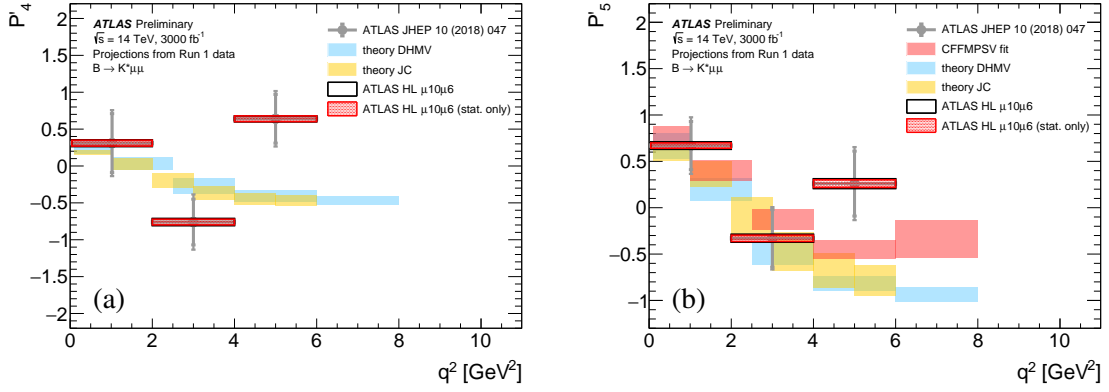


Figure 3: Projected ATLAS HL-LHC measurement precision in the P'_4 (a) and P'_5 (b) parameters for the intermediate $\mu 10\mu 6$ trigger scenario compared to the ATLAS Run 1 measurement. Alongside, theory predictions (CFFMPSV [7], DHMV [8] and JC [9, 10]) are also shown. Both the projected statistical and the total (statistical and systematic) uncertainties are shown. While the HL-LHC toy-MC were generated with the DHMV central values of the P'_4 and P'_5 parameters, in these plots the central values are moved to the ATLAS Run 1 measurement for better visualization of the improvement in the precision [20].

4. High-Luminosity LHC Prospects

At the High-Luminosity LHC (HL-LHC), due to a new all-silicon Inner Tracker (ITk) the mass resolution of the 4-prong FCNC decay $B_d^0 \rightarrow K^{*0} \mu^+ \mu^-$ is expected to improve by 30% with respect to the Run 1 measurement which is used as a baseline for the HL-LHC projections of the measurement. For the HL-LHC case three potential trigger scenarios are considered: two muons with $p_T > 10$ GeV (“conservative”), one muon with $p_T > 10$ GeV and another with $p_T > 6$ GeV (“intermediate”) as well as two muons with $p_T > 6$ GeV (“high yield”) providing 50, 160 and 250 times the Run 1 statistics, respectively. This includes a factor 1.7 due to the increase of the b production cross-section as the center-of-mass energy of the pp collisions rises from 8 TeV to 14 TeV. Estimates for the achievable experimental precision are obtained from pseudo-MC experiments based on the Run 1 signal and background angular distributions and by applying the same fitting procedure as in the Run 1 analysis.

Assuming that the increased statistics will allow for an improved fit model and a better understanding of the exclusive backgrounds, the corresponding systematic uncertainties are scaled by $1/\sqrt{L_{\text{int}}}$. The expected improvement in the measurement accuracy of the P'_4 and P'_5 parameters is demonstrated in Figure 3, compared to the current theoretical predications. Depending on the trigger scenario, the measurement precision for the P'_5 parameter is expected to improve by a factor 5, 8 or 9 relative to the Run 1 measurement.

The branching fraction measurement of the very rare decays $B_s^0 \rightarrow \mu^+ \mu^-$ and $B^0 \rightarrow \mu^+ \mu^-$ will also benefit from the increased statistics and the improved invariant mass resolution at the HL-LHC. The separation of the B_s^0 and B_d^0 mass peaks increases by a factor of 1.65 (1.5) to 2.3σ (1.3σ) in the barrel (end-cap) region compared to Run 1 [21].

The projection of the ATLAS detector performance for measuring $\mathcal{B}(B_{(s)}^0 \rightarrow \mu^+ \mu^-)$ with the expected datasets during the full LHC Run 2 (130 fb^{-1}) and at the HL-LHC (3000 fb^{-1}) [22] us-

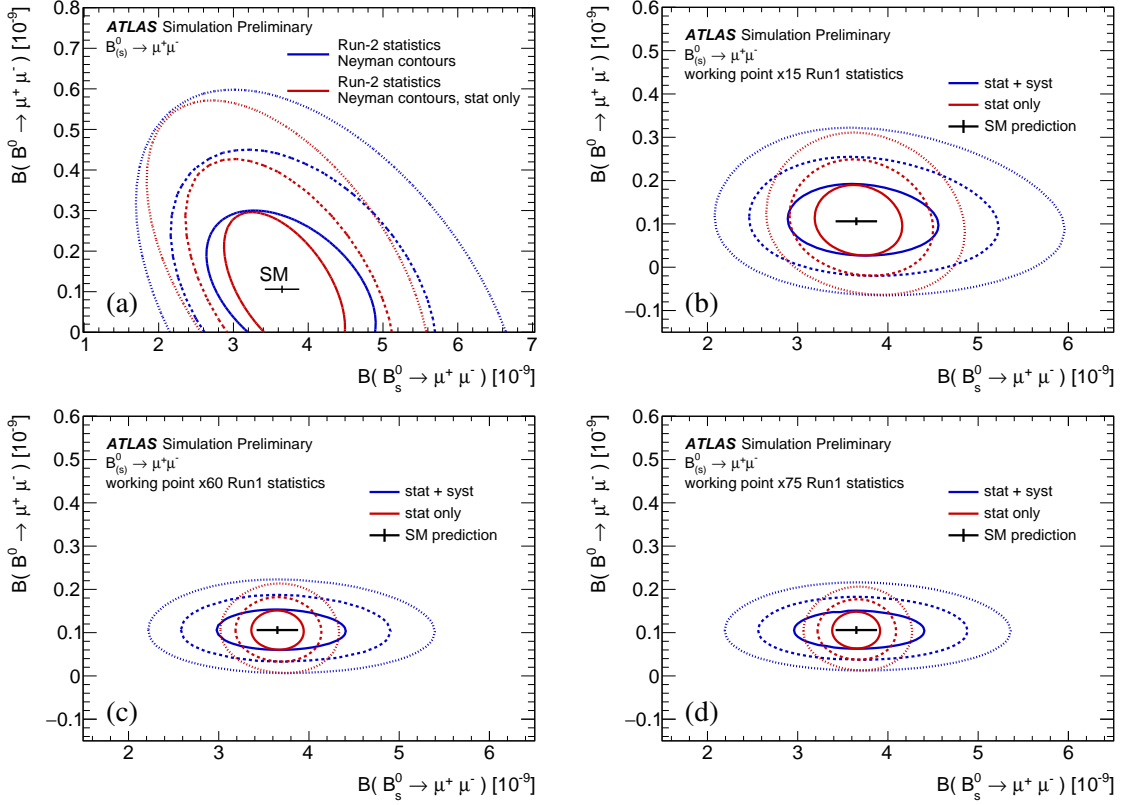


Figure 4: (a): Comparison of 68.3% (solid), 95.5% (dashed) and 99.7% (dotted) confidence level contours obtained exploiting the 2D Neyman belt construction for the full LHC Run 2 case [22]. Red contours are statistical only; blue contours include systematics uncertainties from the ATLAS Run 1 analysis [15] extrapolated to Run 2 statistics. The black points show the SM theoretical prediction and its uncertainty [13]. (b) – (d): Comparison of confidence level profiled likelihood ratio contours for (b) the “conservative”, (c) the “intermediate” and (d) the “high-yield” HL-LHC extrapolation with $\times 15$, $\times 60$ and $\times 75$ the Run 1 statistics for the (10 GeV, 10 GeV), the (6 GeV, 10 GeV) and the (6 GeV, 6 GeV) dimuon trigger scenarios, respectively [22].

ing pseudo-MC experiments is based on the likelihood of the Run 1 analysis. The signal statistics estimate for the Run 2 scenario applies scaling factors for the integrated luminosity, the cross-section increase due to the higher center-of-mass energy of 13 TeV and the muon pair selection with topological triggers with $(p_T(\mu_{1,2}) > 6 \text{ GeV})$ or $(p_T(\mu_1) > 6 \text{ GeV}, p_T(\mu_2) > 4 \text{ GeV})$ thresholds resulting in 7 times the number of signal events in Run 1. The contours of the 2-dimensional Neyman construction (Figure 4 (a)) include the external systematic uncertainties on the b -quark fragmentation fractions f_s/f_d and $\mathcal{B}(B^\pm \rightarrow J/\psi K^\pm)$ which were kept the same as in the Run 1 analysis as well as internal ones like the fit shapes and efficiencies which were scaled according to the increase in statistics. For the HL-LHC case the same three potential trigger scenarios as for the $B_d^0 \rightarrow K^{*0} \mu^+ \mu^-$ analysis are considered resulting in 15 (“conservative”), 60 (“intermediate”) and 75 (“high yield”) times the Run 1 statistics, respectively. The profile likelihood contours of pseudo-experiments based again on the likelihood of the Run 1 analysis demonstrate the increased sensitivity of the ATLAS detector for $\mathcal{B}(B_s^0 \rightarrow \mu^+ \mu^-)$ and $\mathcal{B}(B^0 \rightarrow \mu^+ \mu^-)$ at the HL-LHC (Fig-

ure 4 (b) – (d)). The uncertainty on the f_s/f_d value, conservatively taken as 8.3% from the ATLAS measurement [23], dominates the systematic uncertainty contributions on $\mathcal{B}(B_s^0 \rightarrow \mu^+ \mu^-)$.

5. Summary

Measurements of semi-rare flavor-changing neutral-current decays and of very rare decays, both sensitive to New Physics, by the ATLAS collaboration at the LHC have been presented.

The results of the angular analysis of the $B_d^0 \rightarrow K^{*0} \mu^+ \mu^-$ decay with 20.3 fb^{-1} of Run 1 data agree well with the theoretical predictions in the SM and other measurements, with the largest deviation from theory ($\sim 2.7 \sigma$) observed for the P'_4 and P'_5 parameters in the $q^2 \in [4.0, 6.0] \text{ GeV}^2$ bin.

The results for $\mathcal{B}(B_s^0 \rightarrow \mu^+ \mu^-)$ and the search for the decay $\mathcal{B}(B^0 \rightarrow \mu^+ \mu^-)$ with 36.2 fb^{-1} of Run 2 data agree with the Standard Model and other measurements. There is no sign for the decay $B^0 \rightarrow \mu^+ \mu^-$ in ATLAS data, but ATLAS will add the data taken in 2017 and 2018 to the analysis ($\sim 107 \text{ fb}^{-1}$).

Both analyses will profit considerably from the increased statistics expected from the 3000 fb^{-1} of HL-LHC data as well as detector improvements providing better mass and proper decay time resolutions. This will allow more stringent tests of the Standard Model.

Acknowledgments

This work was partially supported by grants of the German Federal Ministry of Education and Research (BMBF) and the German Helmholtz Alliance “Physics at the Terascale”.

References

- [1] ATLAS Collaboration, *The ATLAS Experiment at the CERN Large Hadron Collider*, 2008 JINST 3 S08003
- [2] L. Evans and P. Bryant (editors), *LHC Machine*, 2008 JINST 3 S08001
- [3] G. Apollinari, I. Béjar Alonso, O. Brüning, P. Fessia, M. Lamont, L. Rossi, L. Taviani (editors), *High-Luminosity Large Hadron Collider (HL-LHC), Technical Design Report V. 0.1*, CERN Yellow Reports Vol. 4/2017, CERN-2017-007-M (CERN, Geneva, 2017) [<https://cds.cern.ch/record/2284929>]
- [4] LHCb Collaboration, *Angular analysis of the $B_d^0 \rightarrow K^{*0} \mu^+ \mu^-$ decay using 3 fb^{-1} of integrated luminosity*, JHEP 02 (2016) 104 [[arXiv:1512.04442](https://arxiv.org/abs/1512.04442)]
- [5] ATLAS Collaboration, *Angular analysis of the $B_d^0 \rightarrow K^{*0} \mu^+ \mu^-$ decay using 3 fb^{-1} of integrated luminosity*, JHEP 10 (2018) 047 [[arXiv:1805.04000](https://arxiv.org/abs/1805.04000)]
- [6] LHCb Collaboration, *Measurement of Form-Factor Independent Observables in the Decay $B_d^0 \rightarrow K^{*0} \mu^+ \mu^-$* , Phys. Rev. Lett. 111 (2013) 191801 [[arXiv:1308.1707](https://arxiv.org/abs/1308.1707)]
- [7] M. Ciuchini et al., *$B \rightarrow K^* \ell^+ \ell^-$ decays at large recoil in the Standard Model: a theoretical reappraisal*, JHEP 06 (2016) 116, [[arXiv:1512.07157](https://arxiv.org/abs/1512.07157)]
- [8] S. Descotes-Genon et al., *On the impact of power corrections in the prediction of $B \rightarrow K^* \mu^+ \mu^-$ observables*, JHEP 12 (2014) 125, [[arXiv:1407.8526](https://arxiv.org/abs/1407.8526)]

- [9] S. Jäger and J. Martin Camalich, *On $B \rightarrow V\ell^+\ell^-$ at small dilepton invariant mass, power corrections and new physics*, *JHEP* **05** (2013) 043 [[arXiv:1212.2263](#)]
- [10] S. Jäger and J. Martin Camalich, *Reassessing the discovery potential of the $B \rightarrow K^*\ell^+\ell^-$ decays in the large-recoil region: SM challenges and BSM opportunities*, *Phys. Rev. D* **93** (2016) 014028 [[arXiv:1412.3183](#)]
- [11] CMS Collaboration, *Measurement of angular parameters from the decay $B_d^0 \rightarrow K^{*0}\mu^+\mu^-$ in proton-proton collisions at $\sqrt{s} = 8$ TeV*, *Phys. Lett. B* **781** (2018) 517 [[arXiv:1710.02846](#)]
- [12] Belle Collaboration, *Angular analysis of $B^0 \rightarrow K^*(892)^0\ell^+\ell^-$* , BELLE-CONF-1603 [[arXiv:1604.04042](#)]
- [13] C. Bobeth et al., *$B_{s,d}^0 \rightarrow \ell^+\ell^-$ in the Standard Model with Reduced Theoretical Uncertainty*, *Phys. Rev. Lett.* **112** (2014) 101801 [[arXiv: 1311.0903](#)]
- [14] M. Beneke, C. Bobeth and R. Szafron, *Power-enhanced leading-logarithmic QED corrections to $B_q \rightarrow \mu^+\mu^-$* , *JHEP* **10** (2019) 232 [[arXiv:1908.07011](#)]
- [15] ATLAS Collaboration, *Study of the rare decays of B_s^0 and B_d^0 into muon pairs from data collected during the LHC Run 1 with the ATLAS detector*, *Eur.~Phys.~J.~C* (2016) 76:513 [[arXiv:1604.04263](#)]
- [16] CMS and LHCb Collaborations, *Observation of the rare $B_s^0 \rightarrow \mu^+\mu^-$ decay from the combined analysis of CMS and LHCb data*, *Nature*, **522** 68-72, 2015 [[arXiv:1411.4413](#)]
- [17] LHCb Collaboration, *Measurement of the $B_s^0 \rightarrow \mu^+\mu^-$ Branching Fraction and Effective Lifetime and Search for $B^0 \rightarrow \mu^+\mu^-$ Decays*, *Phys.~Rev.~Lett.* **118** (2017) 191801 [[arXiv:1703.05747](#)]
- [18] CMS Collaboration, *Measurement of properties of $B_s^0 \rightarrow \mu^+\mu^-$ decays and search for $B^0 \rightarrow \mu^+\mu^-$ with the CMS experiment*, submitted to JHEP, CMS-PAS-BPHY-16-004 [[arXiv:1910.12127](#)]
- [19] ATLAS Collaboration, *Study of the rare decays of B_s^0 and B_d^0 mesons into muon pairs using data collected during 2015 and 2016 with the ATLAS detector*, *JHEP* **04** (2019) 098 [[arXiv:1812.03017](#)]
- [20] ATLAS Collaboration, *$B_d^0 \rightarrow K^{*0}\mu^+\mu^-$ angular analysis prospects with the ATLAS detector at the HL-LHC*, ATL-PHYS-PUB-2019-003, [<https://cds.cern.ch/record/2654519>]
- [21] ATLAS Collaboration, *Expected performance for an upgraded ATLAS detector at High-Luminosity LHC*, ATL-PHYS-PUB-2016-026 [<https://cds.cern.ch/record/2223839>]
- [22] ATLAS Collaboration, *Prospects for the $\mathcal{B}(B_{(s)}^0 \rightarrow \mu^+\mu^-)$ measurements with the ATLAS detector in Run 2 LHC and HL-LHC data campaigns*, ATL-PHYS-PUB-2018-005, [<https://cds.cern.ch/record/2317211>]
- [23] ATLAS Collaboration, *Determination of the ratio of b-quark fragmentation fractions f_s/f_d in pp collisions at $\sqrt{s} = 7$ TeV with the ATLAS detector*, *Phys. Rev. Lett.* **115**, 262001 (2015) [[arXiv:1507.08925](#)]